Electronic Supplementary Material (ESI) for Environmental Science: Nano.

Supporting Information

Defining silica-water interfacial chemistry under nanoconfinement using lanthanides

A.G. Ilgen*[1], N. Kabengi[2], K. Leung[1], P. Ilani-Kashkouli[2], A.W. Knight[3], and L. Loera[1]

1. Sandia National Laboratories, Geochemistry Department, PO Box 5800 Mailstop 0754, Albuquerque, NM 87185-0754, United States
2. Department of Geosciences, Georgia State University, Atlanta, GA, United States
3. Sandia National Laboratories, Storage and Transportation Technologies Department, PO Box 5800 Mailstop 0754, Albuquerque, NM 87185-0754, United States

*Corresponding author. E-mail agilgen@sandia.gov

Pages: 4
Figures: 1
Tables: 4

Geometry of porous SiO_2 SBA-15

In the batch adsorption experiments we observed that the overall Ln^{3+} uptake was higher for non-porous SiO_2, which we attribute to potential diffusion limitations caused by the geometric constraints. These porous SiO_2 materials consist of long channels, as shown in the transmission electron microscopy (TEM) image in Figure S1. TEM samples were prepared by dissolving the SiO_2 in methanol alcohol and drop-casting the solvent on carbon film. A FEI TitanTM G2 80-200 with a cesium probe corrector operated at 200 kV was used for imaging with an ~0.13 nm electron probe, convergence angle of 18.1 mrad, and current of ~55 pA. Scanning TEM images were recorded by bright-field and high-angle annular dark-field (HAADF) detectors with a collection range of 0-30 mrad and 60-160 mrad, respectively.

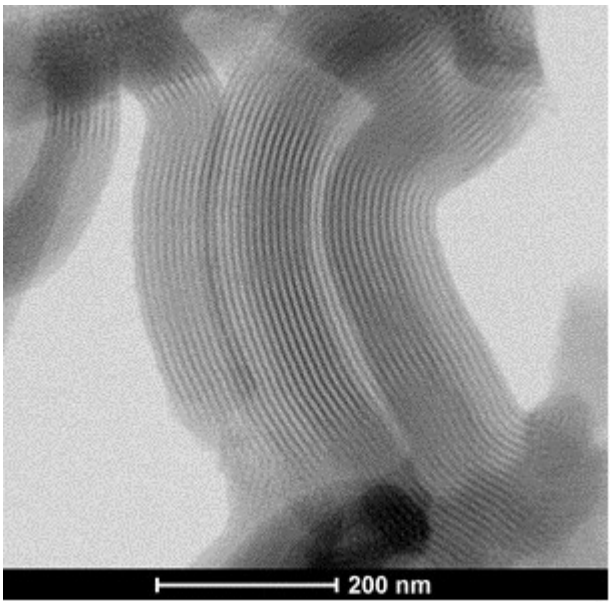

Figure S1. Transmission Electron Microscopy (TEM) micrograph of porous SiO_2 used in the reported experiments.

Summary of K_{ads} values calculated for competitive adsorption experiments

The details regarding the calculation of the K_{ads} values and the trends in the calculated K_{ads} values (Figure 2d-f) are given in the main text. The values used to construct Figure 2d-f are shown below (Table S1), including the ionic radii of the Ln^{3+} of interest,[1] the Ln^{3+} uptake measured in this study, and adsorption equilibrium constant K_{ads} values.

Table S1. Summary of competitive adsorption results, for which Nd^{3+}, Eu^{3+}, Tb^{3+}, Tm^{3+} and Lu^{3+} were all present simultaneously.

Ln^{3+}	Z	Ionic radius	Ln^{3+} uptake $10^{-3} \times$ µmoles·m^{-2}			K_{ads} $10^{-7} \times$ µmoles·m^{-2}		
		Å	SiO_2	SBA-15-4nm	SBA-15-8nm	SiO_2	SBA-15-4nm	SBA-15-8nm
Nd	60	1.175	5.64	1.97	1.34	34.3	6.62	7.32
Nd	60	1.175	3.07	1.63	1.22	17.5	3.98	3.34
Nd	60	1.175	1.04	0.34	0.30	3.91	0.68	0.54
Nd	60	1.175	0.35	0.10	0.08	1.43	0.17	0.22
Eu	63	1.12	7.58	3.23	2.24	46.3	10.8	12.2
Eu	63	1.12	4.40	2.21	1.76	25.1	5.38	4.80
Eu	63	1.12	1.13	0.42	0.35	4.27	0.83	0.63
Eu	63	1.12	0.33	0.09	0.08	1.33	0.16	0.20
Tb	65	1.09	8.36	3.66	2.56	51.1	12.3	14.0
Tb	65	1.09	4.85	2.45	1.96	27.6	5.96	5.36
Tb	65	1.09	1.17	0.45	0.37	4.40	0.89	0.67
Tb	65	1.09	0.34	0.0.9	0.08	1.38	0.15	0.20

Tm	69	1.025	13.37	5.05	4.04	81.7	17.0	22.0
Tm	69	1.025	7.58	2.81	2.42	43.2	6.83	6.60
Tm	69	1.025	1.58	0.54	0.47	5.96	1.08	0.85
Tm	69	1.025	0.34	0.08	0.09	1.38	0.14	0.22
Lu	71	0.995	17.77	6.04	5.19	109	20.3	28.3
Lu	71	0.995	9.11	3.09	2.70	51.9	7.52	7.37
Lu	71	0.995	1.84	0.61	0.54	6.92	1.21	0.97
Lu	71	0.995	0.37	0.11	0.11	1.50	0.18	0.27

X-ray fine structure spectroscopy (XAFS) data fitting

XAFS data analysis results are discussed in the main manuscript text. The fitting parameters obtained during shell-by-shell fitting are shown in Table S2.

Table S2. Summary of X-ray absorption fine structure (XAFS) spectroscopy shell-by-shell fitting results for Nd^{3+}, Tb^{3+}, and Lu^{3+} adsorbed onto non-porous SiO_2 and porous silicas with 4.4 nm and 7.0 nm pores.

Sample	[1] k-range	R-range (Å) uncorr	Shell	[2] CN	[3] R (Å)	[4] σ^2 (Å^2)	[5] ΔE_0 eV	[6] R-factor	[7] Red χ^2	[8] Ind. Pts.
Nd-SiO_2 pH 6	2.0-8.0	1.6-2.2	Nd-O	10(5)	2.50(5)	0.004(10)	4(5)	0.005	26	8
Nd-SBA-7nm pH 6	2.6-9.9	1.7-2.4	Nd-O	10(3)	2.54(3)	0.010(6)	8(3)	0.001	5	10
Nd-SBA-4nm pH 6	2.6-9.9	1.6-2.6	Nd-O	10(3)	2.56(2)	0.006(4)	8(2)	0.039	12	12
Tb-SBA-7nm pH 6	3.6-10.4	1.8-4.0	Tb-O	2(1)	2.22(2)	0.001(2)	5(1)	0.028	5	9
			Tb-O	7(1)	2.42(1)	0.002(1)				
			Tb-Si	2(1)	3.66(2)	0.001(4)				
			Tb-Tb	3(1)	3.75(2)	0.003(2)				
Tb-SBA-4nm pH 6	3.0-10.5	1.8-3.7	Tb-O	3(1)	2.28(2)	0.002(2)	3(2)	0.010	19	17
			Tb-O	7(1)	2.42(2)	0.008(2)				
			Tb-Si	2(2)	3.41(6)	0.01(1)				
			Tb-Tb	3(2)	3.64(6)	0.008(6)				
Lu-SiO_2 pH 6	2.8-11.0	1.6-3.9	Lu-O	4.3(7)	2.13(2)	0.002(2)	7(1)	0.040	14	20
			Lu-O	4.4(8)	2.31(2)	0.002(2)				
			Lu-Si	1(2)	3.33(6)[9]	0.001(7)[9]				
			Lu-Lu	2(2)	3.81(9)	0.002(5)[9]				
			Lu-O	20(9)	3.86(5)	0.023(9)				
Lu-SBA-7nm pH 6	2.8-11.0	1.6-3.9	Lu-O	4.1(6)	2.13(1)	0.001(2)	7(1)	0.018	34	20
			Lu-O	4.3(7)	2.33(1)	0.001(2)				
			Lu-Si	2(5)	3.63(3)	0.02(4)				
			Lu-Lu	5(4)	3.91(5)	0.007(6)				
			Lu-O	14(4)	3.95(3)	0.009(5)				
Lu-SBA-4nm pH 6	2.8-11.0	1.6-3.9	Lu-O	5.2(4)	2.17(1)	0.005(1)	7(1)	0.007	9	20
			Lu-O	3.1(4)	2.35(1)	0.002(2)				

			Lu-Si	2(1)	3.49(5)	0.008(9)				
			Lu-Lu	7(3)	3.93(3)	0.009(4)				
			Lu-O	18(3)	3.96(2)	0.010(2)				
Lu-SBA-4nm pH 4	2.7-11	1.4-2.5	Lu-O	5(2)	2.27(4)	0.003(6)	8(2)	0.012	92	13
			Lu-O	6(2)	2.39(4)	0.003(6)				

Notes:
[1] Usable k-range
[2] Coordination number
[3] Bond length
[4] Debye-Waller factors: mean-square amplitude reduction factor, including thermal and static disorder components
[5] Energy shift between the theoretical and measured spectrum

$$R_{factor} = \frac{\sum_i (data_i - fit_i)^2}{\sum_i data_i^2}$$

[6] R-factor (mean square misfit)

$$\chi_v^2 = \frac{N_{idp}}{N_{pts}} \sum_i \left(\frac{data_i - fit_i}{\varepsilon_i} \right)^2 / (N_{idp} - N_{var})$$

[7] Reduced chi-square
[8] Independent points (number of data points minus number of variable parameters)
$N_{idp} = N_{pts} - N_{var}$
[9] One sigma value is shown in parenthesis. In all other cases errors at a 95% confidence level (2 sigma) are shown.

Molar enthalpies of adsorption calculated from flow microcalorimetry data

The findings from the flow microcalorimetry experiments are discussed in the main text. We present calculated molar adsorption enthalpies, which are based on the measured heats of adsorption and surface coverages (Table 3S).

Table S3. Summary of flow microcalorimetry data for Nd^{3+}, Tb^{3+}, and Lu^{3+} adsorbed onto non-porous SiO_2 and porous silicas with 4.4 nm and 7.0 nm pores.

Ln^{3+}	**SBA-15 4.4nm**			**SBA-15 7.0nm**			**Non-porous SiO_2**		
	Q[1] mJ/mg	**Uptake** µmol/m²	**δH_{ads}[2]** kJ/mol	**Q** mJ/mg	**Uptake** µmol/m²	**δH_{ads}[2]** kJ/mol	**Q** mJ/mg	**Uptake** µmol/m²	**δH_{ads}[2]** kJ/mol
Lu	0.140	0.009	-26.436	0.075	0.008	-13.742	0.178	0.687	3.348
Tb	0.157	0.012	-21.765	0.177	0.010	-26.638	0.094	0.491	2.473
Nd	0.225	0.004	-87.270	0.184	0.004	-69.565	0.077	0.505	1.977

Notes:
[1] Q-Energy. Typically, errors in Q measurements are 5-10%.
[2] δH_{ads} kJ/mol -Molar enthalpy of adsorption.

Gaussian calculations of ΔG_{hydr} for Nd^{3+} and Lu^{3+} in water

As described in the main text, Gaussian calculations were performed to determine how solvation free energies are expected to change under nanoconfinement. The calculated solvation energies for Nd^{3+} and Lu^{3+} in water with varying dielectric constants (ε) are shown in Table S4.

Table S4. Calculated solvation energies ΔG_{hydr} for Nd^{3+} and Lu^{3+} in pure water with dielectric constants (ε) of 78, 10, and 1.

[1] Neodymium			[2] Lutetium		
ε =78	-35.80 eV	-3454 kJ·mol^{-1}	ε =78	-37.62 eV	-3629 kJ·mol^{-1}
ε =10	-34.78 eV	-3356 kJ·mol^{-1}	ε =10	-36.57 eV	-3528 kJ·mol^{-1}
ε =1	-23.04 eV	-2233 kJ·mol^{-1}	ε =1	-23.94 eV	-2310 kJ·mol^{-1}

Notes:

[1] For Nd^{3+} 9-coordinated water in all cases

[2] For Lu^{3+} 8-coordinated water, except for ε =1, where a 9-coordinated model was used.

Potential Applications

Due to the similarities in their chemistry, the separation of individual Ln^{3+} ions from their aqueous mixtures has been a major technological hurdle, requiring complicated multi-step solvent-extraction schemes. However, the systematic variations in the adsorption of Ln^{3+} ions onto porous silica surfaces and their pore-size dependent behavior (as described in this paper), can be used to efficiently separate individual Ln^{3+} ions, as proposed in our submitted patent application.[2] Porous silicas are not soluble in acidic solutions, which makes them excellent candidate materials for separating individual lanthanides from acidic leachate solutions. The pore-size dependent behavior described in our work can also be used for liquid mining, separating valuable Ln^{3+} ions from geothermal fluids and from the waste fluids created as a byproduct of subsurface energy extraction.

References

1. D'Angelo, P.; Spezia, R. J. C. A. E. J., Hydration of lanthanoids (III) and actinoids (III): an experimental/theoretical saga. **2012,** *18* (36), 11162-11178.
2. Ilgen, A. Systems and Methods for Separating Rare Earth Elements Using Mesoporous Materials. 3/11/2020 Submitted., 2020.